Inorg. Chem. **2004**, *43*, 5159–5167

Photochemistry of the Dinitrosyl Iron Complex $[S_5Fe(NO)_2]^-$ Leading to Reversible Formation of $[S_5Fe(\mu\text{-}S)_2FeS_5]^{2-}$: Spectroscopic Characterization of Species Relevant to the Nitric Oxide Modification and Repair of [2Fe–2S] Ferredoxins

Ming-Li Tsai,[†] Chiao-Chun Chen,[‡] I-Jui Hsu,[§] Shyue-Chu Ke,*[,||] Chung-Hung Hsieh,[†] Kuo-An Chiang,[||] Gene-Hsiang Lee,[§] Yu Wang,*[,§] Jin-Ming Chen,[⊥] Jyh-Fu Lee,[⊥] and Wen-Feng Liaw*[,†]

Department of Chemistry, National Tsing Hua University, Hsinchu 30043, Taiwan, Department of Chemistry, National Changhua University of Education, Changhua, Taiwan, Department of Chemistry, National Taiwan University, Taipei, Taiwan, Department of Physics, National Dong Hwa University, Hualien, Taiwan , and Synchroton Radition Research Center, Hsinchu 30077, Taiwan

Received April 20, 2004

The reaction of [PPN][$Fe(CO)_3(NO)$] and S_8 in a 1:1 molar ratio in THF proceeded to give the dinitrosyl iron complex [PPN][$S_5Fe(NO)_2$] (**1**) and the known [PPN]$_2$[$S_5Fe(\mu\text{-}S)_2FeS_5$] (**2**). EPR signals of g values $g_z = 2.0148$, $g_x = 2.0270$, and $g_y = 2.0485$ at 77 K confirmed the existence of the unpaired electron in compound **1**. The temperature-dependent magnetic moment of complex **1** indicates that the ground state is one unpaired electron with (S_t, S_L) = ($^1/_2$, 1) at very low temperature (S_t is the total spin quantum number of the system; S_L is the sum of the spin quantum numbers of two NO ligands). The O K-edge absorptions of complex **1** and [$(NO)Fe(S_2CNEt_2)_2$] at 532.1 and 532.5 eV are assigned to the transition of 1s → π^*(NO) and 1s → $\pi^*(NO^+)$, respectively. For the electronic structure of the $\{Fe(NO)_2\}$ core, DFT calculations, magnetic susceptibility measurement, EPR, and Fe K-/L-edge XAS spectroscopy of complex **1** lead to a description of $\{Fe^{1+}(^\bullet NO)_2\}^9$. [2Fe–2S] cluster **2** treated with nitric oxide in THF shows that cluster **2** is transformed into the dinitrosyl iron complex **1** identified by IR, UV–vis, and X-ray diffraction analysis. The reaction may be reversed by the photolysis of the THF solution of **1** in the presence of the NO-accepting reagent $[(C_4H_8O)Fe(S,S\text{-}C_6H_4)_2]^-$ to reform **2**. This result demonstrates a successful biomimetic reaction cycle of the degradation and reassembly of [2Fe–2S] cluster $[S_5Fe(\mu\text{-}S)_2FeS_5]^{2-}$ relevant to the repair of nitric oxide-modified [2Fe–2S] ferredoxin by cysteine desulfurase and L-cysteine in vitro.

Introduction

Extensive EPR studies have identified nitrosyl non-heme iron complexes as products from the interaction of NO with several iron−sulfur and other iron-containing proteins.[1−4] Examples of nitric oxide coordination to iron and the spectroscopic signals of dinitrosyl iron complexes (DNICs) are of much interest, particularly in light of their roles in sulfur-rich protein uptake and degradation.[2] Recently, EPR and UV−vis absorption studies demonstrated that mammalian ferrochelatase is strongly inhibited by nitric oxide

* Authors to whom correspondence should be addressed. E-mail: wfliaw@mx.nthu.edu.tw (W.-F.L.); yuwang@xtal.ch.ntu.edu.tw (Y.W.); ke@mail.ndhu.edu.tw (S.-C.K.).
[†] National Tsing Hua University.
[‡] National Changhua University of Education.
[§] National Taiwan University.
[||] National Dong Hwa University.
[⊥] Synchroton Radition Research Center.

(1) (a) Kennedy, M. C.; Antholines, W. E.; Beinert, H. *J. Biol. Chem.* **1997**, *272*, 20340. (b) Morse, R. H.; Chan, S. I. *J. Biol. Chem.* **1980**, *255*, 7876. (c) Drapier, J. C.; Pellat, C.; Henry, Y. *J. Biol. Chem.* **1991**, *266*, 10162. (d) Lee, M.; Arosio, P.; Cozzi, A.; Chasteen, N. D. *Biochemistry* **1994**, *33*, 3679. (e) Lepoivre, M.; Flaman, J.-M.; Bobé, P.; Lemaire, G.; Henry, Y. *J. Biol. Chem.* **1994**, *269*, 21891.

(2) (a) Foster, M. W.; Cowan, J. A. *J. Am. Chem. Soc.* **1999**, *121*, 44093. (b) Butler, A. R.; Megson, I. L. *Chem. Rev.* **2002**, *102*, 1155. (c) Sellers, V. M.; Johnson, M. K.; Dailey, H. A. *Biochemistry* **1996**, *35*, 2699.

(3) (a) Vanin, A. F. *Biochemistry (Moscow)* **1998**, *63*, 782. (b) Wang, P. G.; Xian, M.; Tang, X.; Wu, X.; Wen, Z.; Cai, T.; Janczuk, A. J. *Chem. Rev.* **2002**, *102*, 1091. (c) Vanin, A. F. *Biochemistry (Moscow)* **1995**, *60*, 225. (d) Vanin, A. F.; Malenkova, I. V.; Serezhenkov, V. A. *Nitric Oxide* **1997**, *1*, 191.

(4) Ford, P. C.; Bourassa, J.; Miranda, K.; Lee, B.; Lorkovic, I.; Boggs, S.; Kudo, S.; Laverman, L. *Coord. Chem. Rev.* **1998**, *171*, 185.

10.1021/ic0494915 CCC: $27.50
Published on Web 07/10/2004

Scheme 1. Biological Cycle of Degradation and Reassembly of the Ferredoxin [2Fe−2S] Cluster

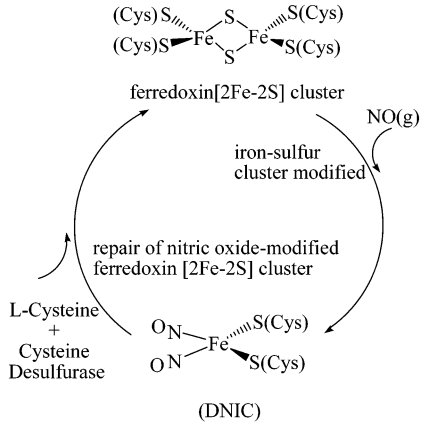

Scheme 2. Biomimetic Degradation and Reassembly of the [2Fe−2S] Cluster $[S5Fe(\mu\text{-}S)_2FeS_5]^{2-}$

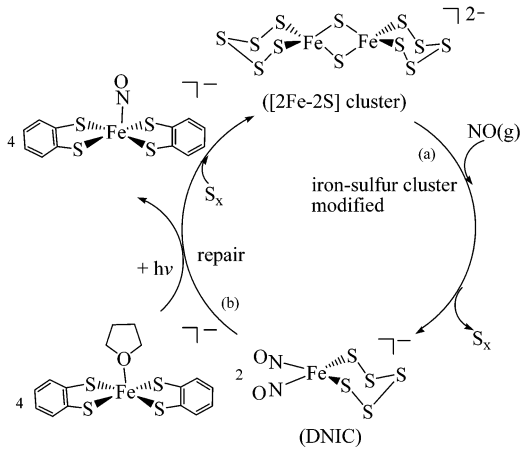

via destruction of the [2Fe−2S] cluster to form a cysteinyl-coordinated monomeric iron dinitrosyl complex.[2c] DNICs have been suggested to be storage sites and transporters of NO in vivo as well as intermediates of the iron-catalyzed degradation and formation of *S*-nitrosothiols.[3,4] In addition, the activation of SoxR protein, a redox-sensitive transcription activator, in *Escherichia coli* on exposure to macrophage-generated NO was suggested to occur through nitrosylation of the [2Fe−2S] clusters to form protein-bound dinitrosyl iron dithiol adducts.[5]

Very recently, Ding and co-workers showed that when *E. coli* cells are exposed to nitric oxide the ferredoxin [2Fe−2S] clusters are modified to form protein-bound dinitrosyl iron complexes. In the repair of the nitric oxide-modified ferredoxin [2Fe−2S] cluster, the dinitrosyl iron complexes can be directly transformed back to the ferredoxin [2Fe−2S] cluster by cysteine desulfurase (IscS) and L-cysteine in vitro with no need for the addition of iron or any other protein components.[6,7] The removal of the dinitrosyl iron complex from ferredoxin and the prevention of the reassembly of the [2Fe−2S] cluster suggests that the iron in the dinitrosyl iron complex may be recycled for the reassembly of the iron−sulfur cluster in the protein.[6,7] The biological cycle of degradation and reassembly of the ferredoxin [2Fe−2S] cluster is shown in Scheme 1.

Glidewell and co-workers reported that reactions of iron−sulfur protein model compounds $[Fe_4S_4(SR)_4]^{2-}$/$[Fe_2(\mu\text{-}S)_2(S,S\text{-}C_6H_4)_2]^{2-}$ and nitric oxide/nitrite, followed by the acidic workup, yielded the anionic $[Fe_4S_3(NO)_7]^-$ via the formation of the paramagnetic intermediate $[(NO)_2Fe(SH)_2]^-$.[8] In addition, Roussin's black salt $[Fe_4S_3(NO)_7]^-$ was reported to be isolated upon reaction of $[Fe(CO)_3(NO)]^-$ with elemental sulfur or polysulfide[9] and also upon protonation of $[Fe_2S_2(NO)_4]^{2-}$ by HBF_4/CF_3COOH.[10] Interestingly, the facile conversion of $[Fe_2S_2(NO)_4]^-$ into $[Fe_4S_3(NO)_7]^-$ was also observed simply by dissolving $[Fe_2S_2(NO)_4]^-$ salt in CH_2Cl_2.[11]

Because of the small energy difference between transition-metal d and NO π^* orbitals,[12] it is complicated to define the "noninnocent" character of NO acting as NO^+, NO^-, or a paramagnetic neutral NO• radical. Thus, the number of electrons in the $M-(NO)_x$ (M = transition metal) unit is generally designated as $\{M(NO)_x\}^n$ according to the Enemark−Feltham notation.[13] The variable nature of the NO ligand from $M-NO^-$ to M−NO• to $M-NO^+$, with the oxidation state of the metal decreasing, determines the reactivity of the nitrosyl ligand. Within the class of DNICs, NO binding to an iron center usually leads to an $\{Fe^{-1}(NO^+)_2\}^9$ or an $\{Fe^{1+}(\bullet NO)_2\}^9$ system.[1,2,13] It is described as an $S = {}^1/_2$ (d^9 Fe(−I)) or an $S = {}^3/_2$ (d^7 Fe(I)) center that is antiferromagnetically coupled to two NO• radicals ($S = {}^1/_2$), respectively. The oxidation states of the iron and NO in these complexes are still in controversy, though it is generally believed that the iron was formally present as d^9 Fe(−1) on the basis of the linear Fe−N−O bond angles proposed to exist as NO^+.[2b,3,13]

In this study, XAS, SQUID, DFT calculations, and EPR spectroscopy were used to study the electronic structure of the $\{Fe(NO)_2\}^9$ unit of complex $[S_5Fe(NO)_2]^-$ (**1**) and to assign the formal oxidation states of the Fe and NO units in complex **1**. Also reported here is the example of biomimetic degradation and reassembly of the [2Fe−2S] cluster. As shown in Scheme 2, a biomimetic reaction cycle, analogous to the biological cycle (Scheme 1) of the L-cysteine-mediated removal of the dinitrosyl iron complexes from proteins and the degradation/reassembly of the [2Fe−2S] clusters in proteins, was drawn on the basis of the model compound study.

(5) Ding, H.; Demple, B. *Proc. Natl. Acad. Sci. U.S.A.* **2000**, *97*, 5146.
(6) Rogers, P. A.; Ding, H. *J. Biol. Chem.* **2001**, *276*, 30980−30986.
(7) Yang, W.; Rogers, P. A.; Ding, H. *J. Biol. Chem.* **2002**, *277*, 12868−12873.
(8) (a) Butler, A. R.; Glidewell, C.; Li, M.-H. *Adv. Inorg. Chem.* **1988**, *32*, 335. (b) Butler, A. R.; Glidewell, C.; Hyde, A. R.; Walton, J. C. *Inorg. Chim. Acta* **1985**, L7.
(9) Butler, A. R.; Glidewell, C.; Hyde, A. R.; Walton, J. C. *Polyhedron* **1985**, *4*, 797.
(10) Beck, W.; Grenz, R.; Götzfried, F.; Vilsmaier, E. *Chem. Ber.* **1981**, *114*, 3184.
(11) Butler, A. R.; Glidewell, C.; Hyde, A. R.; McGinnis, J. *Inorg. Chem.* **1985**, *24*, 2931.
(12) (a) Franz, K. J.; Lippard, S. J. *J. Am. Chem. Soc.* **1998**, *120*, 9034. (b) Brown, C. A.; Pavlosky, M. A.; Westre, T. E.; Zhang, Y.; Hedman, B.; Hodgson, K. O.; Solomon, E. I. *J. Am. Chem. Soc.* **1995**, *117*, 715. (c) Mingos, D. M. P.; Sherman, D. J. *Adv. Inorg. Chem.* **1989**, *34*, 293.
(13) Enemark, J. H.; Feltham, R. D. *Coord. Chem. Rev.* **1974**, *13*, 339.

Scheme 3

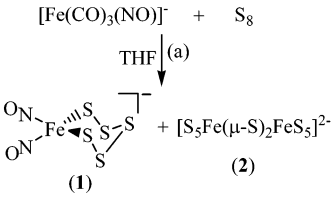

Results and Discussion

As presented in Scheme 3, a straightforward synthetic reaction of [PPN][Fe(CO)$_3$(NO)] with 1 equiv of S_8 in THF at ambient temperature was conducted. In contrast to the formation of $[(NO)_2Fe(SH)_2]^-$, the ($[Fe_4S_3(NO)_7]^-$) compound observed by Glidewell and co-workers for the reaction of S_8/S_x^{2-} and $[Fe(CO)_3(NO)]^-$,[8,9] the reaction mixture finally led to the isolation of the THF-soluble dark-brown [PPN]-$[S_5Fe(NO)_2]$ (**1**) and the known red-brown $[PPN]_2[S_5Fe(\mu\text{-}S)_2FeS_5]$ (**2**) precipitate identified by IR ν_{NO} and X-ray diffraction analysis.[15,16] Complex **1** exhibits two IR ν_{NO} bands (1739 s, 1695 s cm^{-1} (THF)). The ν_{NO} bands of complex **1** are 5 and 2 cm^{-1} lower than those of the dinitrosyl iron−chalcogenolate complexes $[(NO)_2Fe(SPh)_2]^-$ (1744, 1709 cm^{-1} (CsI))[17] and $[(NO)_2Fe(SePh)_2]^-$ (1741 s, 1697 s cm^{-1} (CH_2Cl_2)),[18,19] respectively. Thus, we propose that the $[S_5]^{2-}$ unit, $[SePh]_2^{2-}$, and $[SPh]_2^{2-}$ have similar electron-donating abilities to the $\{Fe(NO)_2\}^9$ moiety.[13,19] This formalism invokes the Enemark−Feltham notation, which stresses the well-known covalency and delocalization in the electronically amorphous $Fe(NO)_2$ unit without committing to formal oxidation states of Fe and NO, respectively; that is, the assignment could be $Fe^{I-}(NO^+)_2$, $Fe^I(^\bullet NO)_2$, $Fe^{III}(NO^-)_2$, or a resonance hybrid of these forms.[13]

Upon injecting NO gas into a THF solution of model compound **2**, a rapid reaction ensued over the course of 20 min to give, by what may be described as NO radical coordinative addition to Fe^{3+} and the subsequent reductive elimination of S_x, dark-brown complex **1** after the reaction solution was precipitated by hexane and extracted by THF (Scheme 2a). Direct evidence of the formation of dinitrosyl iron complex **1** through the reaction of complex **2** and NO gas was provided by IR ν_{NO} and UV−vis spectra. Nitric oxide binding to iron results in the degradation of dinuclear iron−sulfide model compound **2** to yield dinitrosyl iron complex **1**,[2,3] as observed in ferrochelatase, which is inhibited by nitric oxide and, in SoxR, is activated by NO to result in the destruction of the [2Fe−2S] clusters yielding mononuclear DNICs.[2c,5]

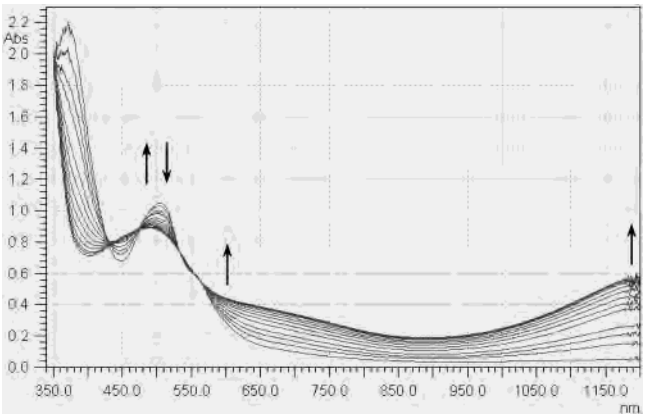

Figure 1. Spectral changes demonstrate the growth of $[(NO)Fe(S,S\text{-}C_6H_4)_2]^-$ bands (497, 610, and 1190 nm) at the expense of the disappearance of the $[(C_4H_8O)Fe(S,S\text{-}C_6H_4)_2]^-$ band (505 nm) during irradiation (λ_{irr} = 352 nm) of a THF solution of complex **1** in the presence of NO-receptor reagent $[(C_4H_8O)Fe(S,S-C_6H_4)_2]^-$. The spectra were recorded at intervals of 10 s. The concentration of complex **1** is 2.857×10^2 μM.

Scheme 4

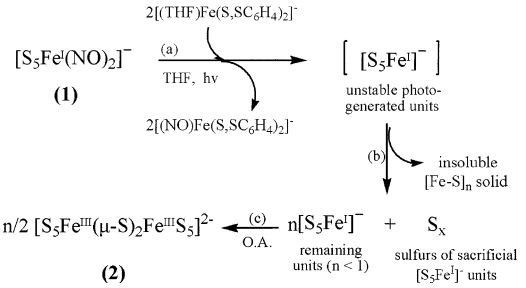

Of importance is that the conversion of dinitrosyl iron complex **1** to [2Fe−2S] cluster **2** was displayed when the THF solution of complex **1** and 2 equiv of NO-acceptor reagent $[(C_4H_8O)Fe(S,S\text{-}C_6H_4)_2]^-$ was photolyzed at ambient temperature (Scheme 2b). Complex $[(C_4H_8O)Fe(S,S\text{-}C_6H_4)_2]^-$ has a band in the electronic absorption spectrum at 505 nm (THF). Upon photolysis of a THF solution of complex **1** and 2 equiv of $[(C_4H_8O)Fe(S,S\text{-}C_6H_4)_2]^-$ at room temperature, the color of the solution changed from dark brown to reddish brown (signifying the formation of $[(NO)Fe(S,S\text{-}C_6H_4)_2]^-$) accompanied by a red-brown precipitate (complex **2**), where the band at 505 nm disappeared with the formation of one absorption band at 497 nm ($[(NO)Fe(S,S\text{-}C_6H_4)_2]^-$ in THF) (Figure 1).[14] The red-brown precipitate, complex **2**, was isolated in 35% yield after the reaction solution was separated and recrystallized with CH_2Cl_2. The reformation of complex **2** under these conditions may be accounted for by the following reaction sequence: NO scavenging by $[(C_4H_8O)Fe(S,S\text{-}C_6H_4)_2]^-$ leading to the buildup of unstable, photogenerated $[S_5Fe^I]$ units, followed by the reduction of two sulfurs atoms of the sacrificial $[S_5Fe^I]$ unit providing inorganic sulfide for the reassembly of complex **2** from the remaining $[S_5Fe^I]$ (Scheme 4). In contrast, irradiation of the THF solution of complex **1** in the absence of NO-acceptor reagent $[(C_4H_8O)Fe(S,S\text{-}C_6H_4)_2]^-$ for 10 min gave only a trace of an insoluble yellow solid. Thus, the presence of NO-acceptor reagent $[(C_4H_8O)Fe(S,S\text{-}C_6H_4)_2]^-$ appears to be crucial in triggering the repair of dinitrosyl iron complex **1** back to [2Fe−2S] cluster **2**.

(14) (a) Lee, C.-M.; Hsieh, C.-H.; Dutta, A.; Lee, G.-H.; Liaw, W.-F. *J. Am. Chem. Soc.* **2003**, *125*, 11492. (b) Ileperuma, O. A.; Feltham, R. D. *Inorg. Chem.* **1975**, *14*, 3042.
(15) (a) Coucouvanis, D.; Swenson, D.; Stremple, P.; Baenziger, N. C. *J. Am. Chem. Soc.* **1979**, *101*, 3392. (b) Strasdeit, H.; Krebs, B.; Henkel, G. *Inorg. Chim. Acta* **1984**, *89*, L11.
(16) Hayton, T. W.; Legzdins, P.; Sharp, W. B. *Chem. Rev.* **2002**, *102*, 935.
(17) Strasdeit, H.; Krebs, B.; Henkel, G. *Z. Naturforsch., B: Chem. Sci.* **1986**, *41*, 1357.
(18) Liaw, W.-F.; Chiang, C.-Y.; Lee, G.-H.; Peng, S.-M.; Lai, C.-H.; Darensbourg, M. Y. *Inorg. Chem.* **2000**, *39*, 480.
(19) Coucouvanis, D.; Stremple, P.; Simhon, E. D.; Swenson, D.; Baenziger, N. C.; Draganjac, M.; Chan, L. T.; Simopoulos, A.; Papaefthymiou, V.; Kostikas, A.; Petrouleas, V. *Inorg. Chem.* **1983**, *22*, 293.

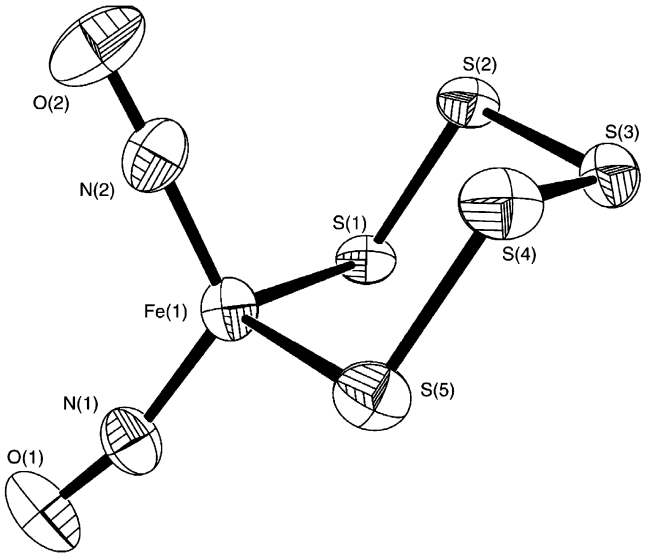

Figure 2. ORTEP drawing and labeling scheme of the $[S_5Fe(NO)_2]^-$ anion with thermal ellipsoids drawn at 50% probability.

Table 1. Selected Bond Distances (Å) and Angles (deg) of Complex **1**

Fe−N(1)	1.686(2)	Fe−N(2)	1.670(3)
Fe−S(1)	2.2877(8)	Fe−S(5)	2.2874(8)
N(1)−O(1)	1.177(3)	N(2)−O(2)	1.178(3)
S(1)−S(2)	2.0573(9)	S(2)−S(3)	2.0556(10)
S(3)−S(4)	2.0502(11)	S(4)−S(5)	2.0536(11)
S(1)−Fe−S(5)	107.68(3)	N(1)−Fe−N(2)	119.69(12)
S(1)−Fe−N(2)	102.67(9)	N(1)−Fe−S(1)	109.82(8)
N(2)−Fe−S(5)	111.51(9)	O(1)−N(1)−Fe	165.9(2)
O(2)−N(2)−Fe	172.8(2)	S(1)−S(2)−S(3)	104.95(4)
S(2)−S(3)−S(4)	106.50(4)	S(3)−S(4)−S(5)	106.32(4)

Structure. Anionic complex **1**, Figure 2, adopts a distorted tetrahedral structure. The nitrosyls are slightly bent (∠Fe−N(1)−O(1) = 165.9(2)° and ∠Fe−N(2)−O(2) = 172.8(2)°) and flared toward each other (O(1)−Fe−O(2) = 103.4° vs N(1)−Fe−N(2) = 115.6°; attracto conformation) (Table 1).[21] The X-ray structural determination of complex **1** shows that the FeS_5 ring is in the chair conformation, similar to those found in complex **2**, $[S_5FeWS_4]^{2-}$,[19] and Cp_2TiS_5.[22] The mean value of the Fe−S bond length in complex **1** is 2.2876(8) Å, slightly shorter than those in complex **2**, 2.323(2) Å (2.321(3) Å in $[Ph_4P]_2[Fe_2S_{12}]$).[15] The average S−S bond length of 2.054(1) Å in complex **1** (spanning the range from 2.0502(11) to 2.0573(9) Å) is slightly shorter than that (2.065(2) Å) in complex **2**.

EPR Spectroscopy. At 4.2 K, complex **1** exhibits an $S = {}^1/_2$, rhombic EPR spectrum (Figure 3A, top) with principal g values at $g_z = 2.0148$, $g_x = 2.0270$, and $g_y = 2.0485$ similar to those of the tetrahedral $[(NO)_2Fe(SR)_2]^-$ complex suggestive of a $\{Fe(NO)_2\}^9$ configuration.[23] At room temperature, the anisotropy of the g factor is averaged out because of the fast tumbling of the molecule and yields an isotropic $g = 2.03$ signal characteristic of low-molecular-weight dinitrosyl iron thiol complexes (Figure 3B, bottom).[2,3,5,7]

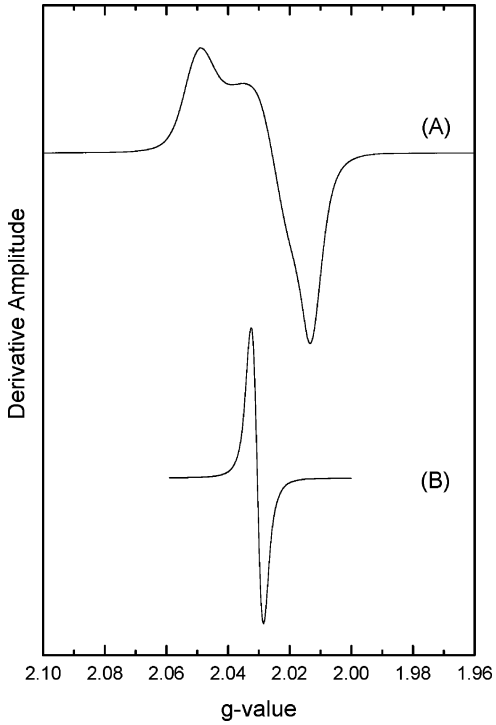

Figure 3. X-band EPR spectra of complex **1** (A) frozen in THF and (B) measured at room temperature.

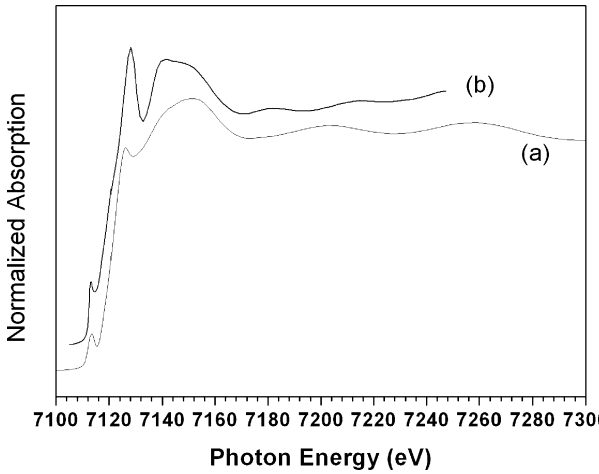

Figure 4. Fe K-edge spectra of complex **1** from (a) experiment (b) simulation.

X-ray Absorption Spectroscopy. To clarify the detailed electronic structure of the $\{Fe(NO)_2\}$ core of complex **1**, we made X-ray absorption measurements. The experimental and theoretical simulation Fe K-edge spectra are depicted in Figure 4a and b, respectively. In comparison with the simulated spectra and projected DOS (density of state) done by FEFF82,[32] the preedge transition is due to not only the

(20) (a) Chu, C. T.-W.; Dahl, L. F. *Inorg. Chem.* **1977**, *16*, 3245. (b) Scott, M. J.; Holm, R. H. *Angew. Chem., Int. Ed. Engl.* **1993**, *32*, 564.
(21) Richter-Addo, G. B.; Legzdins, P. *Metal Nitrosyls*; Oxford University Press: New York, 1992; p 81.
(22) (a) Muller, A.; Diemann, E. *Adv. Inorg. Chem.* **1987**, *31*, 89. (b) Draganjac, M.; Rauchfuss, T. B. *Angew. Chem., Int. Ed. Engl.* **1985**, *24*, 742.
(23) Costanzo, S.; Ménage, S.; Purrello, R.; Bonomo, R. P.; Fontecave, M. *Inorg. Chim. Acta* **2001**, *318*, 1.
(24) Goodman, B. A.; Raynor, J. B.; Symons, M. C. R. *J. Chem. Soc. A* **1969**, 2572.
(25) (a) Gibson, J. F. *Nature* **1962**, *196*, 64. (b) McDonald, C. C.; Phillips, W. D.; Mower, H. F. *J. Am. Chem. Soc.* **1965**, *87*, 3319.
(26) Li, Ming; Bonnet, D.; Bill E.; Neese, F.; Weyhermüller, T.; Blum, N.; Sellmann, D.; Wieghardt, K. *Inorg. Chem.* **2002**, *41*, 3444.
(27) Boese, M.; Mordvintcev, P. I.; Vanin, A. F.; Büsse, R.; Mülsch, A. *J. Biol. Chem.* **1995**, *270*, 29244.

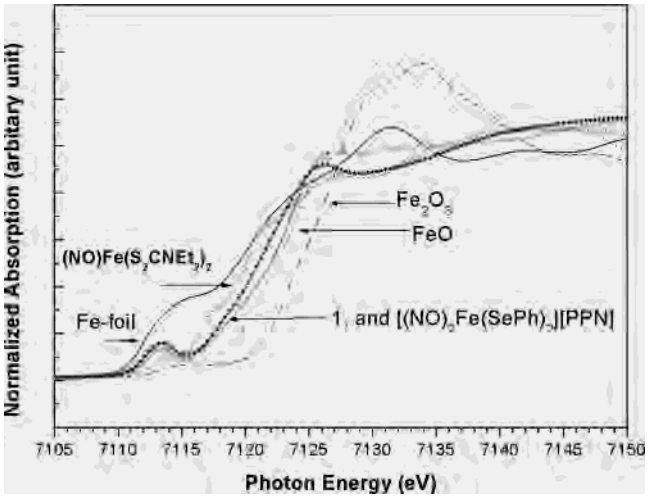

Figure 5. Fe K-edge spectra of Fe foil, $[(NO)Fe(S_2CNEt_2)_2]$, FeO, Fe_2O_3, $[(NO)_2Fe(SePh)_2]^-$, and complex **1**.

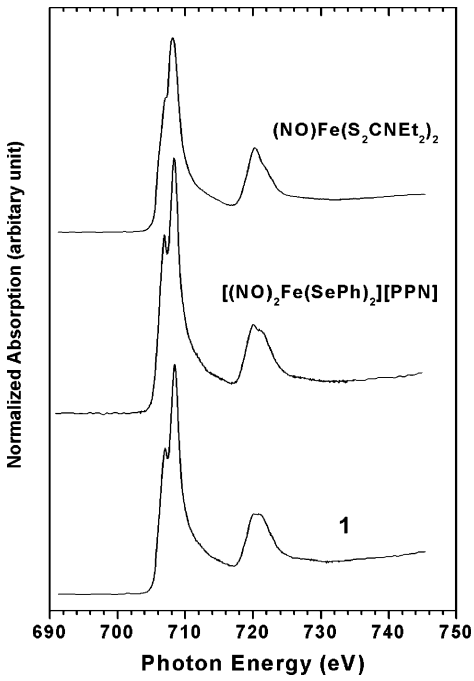

Figure 6. Fe $L_{III,II}$-edge spectra of complex **1** and two other related iron nitrosyl complexes.

symmetry allowed in the distorted T_d local environment of the Fe center but also the d−p mixing between Fe and ligand atoms. The absorption around 7127 eV is assigned to the dipole transition between 1s (Fe) and 4p (Fe) orbitals. The Fe K- and $L_{III,II}$ -edge spectra together with some reference compounds are depicted in Figures 5 and 6, respectively. The spectra indicate that the oxidation state of Fe in complex **1** is roughly the same as that in $[(NO)_2Fe(SePh)_2][PPN]$ in

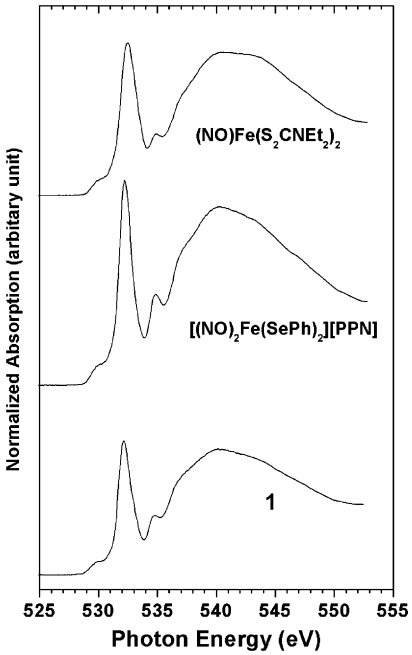

Figure 7. O K-edge spectra of the three Fe complexes that are indicated in Figure 6.

terms of the near-edge spectra of Fe K- and $L_{III,II}$-edge absorptions. This is also consistent with the similarity of the electron-donating ability of $[S_5]^{2-}$, $[SePh]_2^{2-}$, and $[SPh]_2^{2-}$ ligands on the basis of the IR measurements. On the basis of the spectra shown in Figure 5, the oxidation state of Fe in complex **1** is definitely higher than that of Fe foil but lower than those of FeO and Fe_2O_3. In addition, the K-edge energy is close to that of $(NO)Fe(S_2CNEt_2)_2$, which is generally known[24,25] as a nitrosyl ligand (NO^+) bound to a low-spin d^7 Fe(I). Thus, the iron metal of complex **1** is best assigned as the Fe(I) oxidation state, and the NO ligands in complex **1** would be in their neutral radical state. Because the NO radical is more electron rich than the NO^+ lignad, the absorption energy of the O or N K-edge spectra should be shifted to a lower-energy position in comparison with thate of nitrosyl (NO^+) in $[(NO)Fe(S_2CNEt_2)_2]$. The O K-edge spectra of complex **1**, $[(NO)Fe(S_2CNEt_2)_2]$, and [PPN]-$[(NO)_2Fe(SePh)_2]$ are displayed in Figure 7. Roughly, the peaks around 532−533 and 538 eV are assigned to transitions 1s → π^* and 1s → σ^*, respectively. The absorption at 532.5 eV in the complex $[(NO)Fe(S_2CNEt_2)_2]$ is assigned to transition 1s → $\pi^*(NO^+)$, and the corresponding absorptions at 532.1 and 532.2 eV belong to complex **1** and [PPN]-$[(NO)_2Fe(SePh)_2]$), respectively. The slightly lower absorption energy is believed to be the 1s → π^*(NO) transition because of the fact that the NO ligand is more electron rich than NO^+. Therefore, the X-ray absorption spectra support the assignment of formal oxidation states Fe(I) and the NO radical in $\{Fe(NO)_2\}$.[9] In other words, the unpaired electrons are located both at NO and Fe, and the spin system could be $(S_t, S_L) = (^5/_2, 1), (^3/_2, 0), (^1/_2, 1)$ with $S = ^3/_2$ of (d^7 Fe-(I)), where S_t is the total spin quantum number of the system and S_L is the sum of the spin quantum number of two NO ligands.

(28) Hedberg, L.; Hedberg, K.; Satija, S. K.; Swanson, B. I. *Inorg. Chem.* **1985**, *24*, 2766.
(29) Works, C. F.; Jocher, C. J.; Bart, G. D.; Bu, X.; Ford, P. C. *Inorg. Chem.* **2002**, *41*, 3728.
(30) Blessing, R. H. *Acta Crystallogr., Sect. A* **1995**, *51*, 33.
(31) Sheldrick, G. M. *SHELXTL, Program for Crystal Structure Determination;* Siemens Analytical X-ray Instruments Inc.: Madison, WI, 1994.
(32) Ankudinov, A. L.; Ravel, B.; Rehr, J. J.; Conradson, S. D. *Phys. Rev. B* **1998**, *58*, 7565.

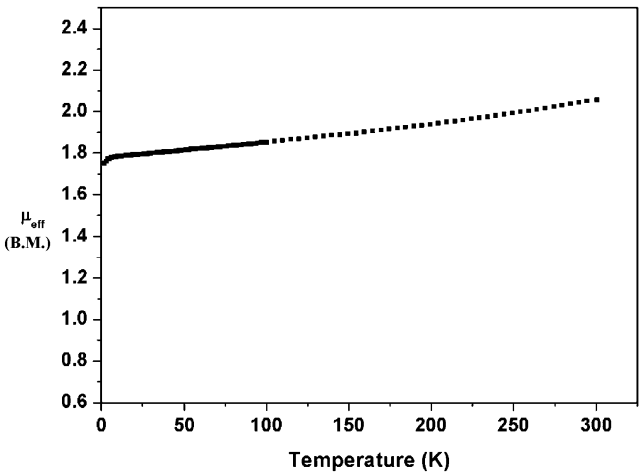

Figure 8. Magnetic moment of complex **1** in the temperature range of 2−300 K.

Magnetic Measurement. The temperature-dependent magnetic moment of complex **1** is shown in Figure 8. The data indicate that the ground state is one unpaired electron with (S_t, S_L) = ($^1/_2$, 1) at very low temperature, which implies antiferromagnetic coupling between Fe and two NO radicals. Although the magnetic moment is slightly temperature-dependent, the contribution of the doublet state remains ~90% even at 300 K. On the basis of EPR, X-ray absorption spectra, and magnetic measurement, the formal oxidation states of Fe/NO in $\{Fe(NO)_2\}^9$ complex **1** are best described as a combination of a d^7 Fe(I) with $S = {}^3/_2$ and two NO radical ligands with $S = {}^1/_2$. Because of the strong bonding between Fe and N, the net unpaired electron is mainly located on the Fe atom.

DFT Computation. To further portray the electronic structure of the $\{Fe(NO)_2\}^9$ motif and to complement experimental data, we have employed a hybrid U-B3LYP density functional calculation of complex **1** with the molecular geometry taken from the diffraction data. The magnetic susceptibility and EPR results at very low temperature ($S = {}^1/_2$) imposed convergence to a doublet state in the SCF calculation.

The orbital energies and the main coefficients for the selected occupied and virtual molecular orbitals (MOs) are shown in Table 3 and Figure 9, respectively. One extra electron is housed in the α manifold. In tetrahedral geometry, all five d orbitals of the metal can interact strongly with both σ and π orbitals of the ligands. The calculation indeed reveals strong covalent interactions between iron and its ligands; as a consequence, the iron-based molecular orbitals have contributions from both NO ligands and the sulfur ring simultaneously (Table 3). Despite this delocalization, we have attributed MO 57α, 58α, 60α, 61α, and 64α (from 43 to 49%) to the atomiclike Fe 3d orbitals. The SOMO is dominated by Fe($d_{x^2-y^2}$) and the S_5 ring.

The spin structure of complex **1** can be derived from the calculated net spin densities. As illustrated in Table 4, the spin density is not only confined to the iron ion but also distributed equally over the two NO ligands. The total calculated molecular spin is one unpaired electron inherited from the imposed convergence to a doublet state in the open-shell spin-unrestricted SCF calculation. The net spin densities of iron and NO have opposite signs. This is a consequence of the significant overlap between Fe 3d and NO $2\pi^*$ orbitals, which gives rise to spin pairing. The net β spin density at each NO ligand (~ −0.94) is equivalent to 1 unit of molecular spin that corresponds to an idealized NO radical configuration ($S = {}^1/_2$). This result supports the $\{Fe^{1+}(^{\cdot}NO)_2\}^9$ electronic configuration.

The α spin is predominately located on the Fe (85%), but 14% is equally distributed onto the adjacent S1 and S5. However, the net α spin density from S1, S5, and Fe is 2.84 units and approaches an idealized $S = {}^3/_2$ configuration. Although the atomic spin of Fe is not an integer, reflecting the covalent nature of the molecular environment, the effective atomic spin configurations can be related to the promoted ideal spin configuration as "Fe ($S = {}^3/_2$) antiferromagnetically coupled to two NO ($S = {}^1/_2$) ligands" in the $\{Fe^{1+}(\bullet NO)_2\}^9$ unit.

Table 2. Crystallographic Data of Complex **1**

chem formula	$C_{36}H_{30}N_3O_2S_5FeP_2$
fw	814.72
cryst syst	triclinic
space group	$P\bar{1}$
λ, Å(Mo K_α)	0.7107
a, Å	10.5096(1)
b, Å	12.5288(1)
c, Å	15.1664(2)
α, deg	112.0027(5)
β, deg	90.6617(4)
γ, deg	91.1990(4)
V, Å^3	1850.74(3)
Z	2
d_{calcd}, g cm^{-3}	1.462
μ, mm^{-1}	0.813
T, K	150(1)
R	0.0422[a]
$R_w(F^2)$	0.0939[b]
GOF	1.034

[a] $R = \sum |(F_o - F_c)|/\sum F_o$. [b] $R_w(F^2) = \{\sum w(F_o^2 - F_c^2)^2/\sum[w(F_o^2)^2]\}^{1/2}$.

Conclusions and Comments. The reaction of [PPN][Fe(CO)$_3$(NO)] and S_8 in THF resulted in the formation of dinitrosyl iron complex **1** and [2Fe-2S] complex **2**. On the basis of magnetic susceptibility measurements, EPR spectroscopy, DFT calculations, and K, L-edge XAS, it is further inferred that dinitrosyl iron complex **1** is better described as $\{Fe^{1+}(\bullet NO)_2\}^9$ than as $\{Fe^{-1}(NO^+)_2\}$.[9] The degradation of [2Fe−2S] cluster **2** by reaction with NO yields dinitrosyl iron complex **1**. Complex **1** can be converted back to **2** upon photolysis in THF in the presence of NO-acceptor reagent $[(C_4H_8O)Fe(S,S\text{-}C_6H_4)_2]^-$. This reaction cycle (Scheme 2) is similar to the biological cycle (Scheme 1) of the nitric oxide modification and repair of ferredoxin. NO-acceptor complex $[(C_4H_8O)Fe(S,S\text{-}C_6H_4)_2]^-$ is required to promote the transformation of dinitrosyl iron complex **1** to cluster **2** under photolysis.[14] The role of NO-acceptor complex $[(C_4H_8O)Fe(S,S-C_6H_4)_2]^-$ is interpreted as mediating the destabilization of dinitrosyl iron complex **1** under photolysis by scavenging nitric oxide to yield an unstable iron sulfide [S_5-Fe^I] intermediate. Such an intermediate may be recycled for the reassembly of new iron−sulfur clusters, as proposed

Table 3. Orbital Energies and Coefficients as Percentages of Selected MOs[a,b]

MO no.	orbital characters	energy (eV)	coeff			
			Fe (%)	NO (bent)	NO (linear)	S ring
		Unoccupied Levels				
73α	NO ($2\pi^*$) − NO ($2\pi^*$)	1.954	7.3	33.5	40.8	18.5
72α	NO ($2\pi^*$) − Fe (s, d_{yz}) − NO ($2\pi^*$)	1.82	21.9	20.2	41.6	16.3
71β	Fe (d_{z2}) − NO ($2\pi^*$)	1.761	33.6	11.2	18.1	37
70β	NO ($2\pi^*$) − Fe (d_{xy})	1.708	21.2	23.3	8.3	47.2
71α	NO ($2\pi^*$) − Fe (s, d_{xz}) − NO ($2\pi^*$)	1.452	19.6	33.3	18.7	28.5
69β	Fe ($d_{x^2-y^2}$) − NO ($2\pi^*$) − S_5	1.316	31.4	13.7	3.8	51.2
70α	NO ($2\pi^*$) − NO ($2\pi^*$) − S_5	1.315	8.2	40.3	21.2	30.3
		Occupied Levels				
69α	S_5 (HOMO) − Fe ($d_{x^2-y^2}$)	−2.005	19.3	5.5	5.8	69.4
65β	NO ($2\pi^*$) − Fe − NO ($2\pi^*$)	−2.789	19.1	28.5	38.4	13.9
63β	bent NO ($2\pi^*$) − Fe (d_{xy})	−3.387	24.3	43.7	2	30
62β	NO ($2\pi^*$) − Fe (d_{xz}) − NO ($2\pi^*$)	−3.675	20.5	32.4	25.7	21.5
61β	linear NO ($2\pi^*$) − Fe (d_{yz})	−3.845	28.6	9.9	34.3	27.1
64α	Fe (d_{z^2}) − S_5	−4.139	42.9	9.7	17.8	29.6
61α	Fe (d_{yz}) − S_5	−5.569	48.5	1.7	8.5	41.3
60α	Fe (d_{xz}) − S_5	−5.713	44.6	5.6	5.9	43.8
58α	Fe ($d_{x^2-y^2}$) − S_5	−6.143	47.1	3.3	6.7	42.9
57α	Fe (d_{xy}) − S_5	−6.433	42.8	1.5	0.6	55.2
53α	NO (1π) − NO (1π)	−8.995	2.3	38.4	56	3.2
52α	NO (1π) − NO (1π)	−9.182	6.8	16.2	74.4	2.6
51α	NO (1π) − NO (1π)	−9.361	9.4	69.8	19.3	1.6
50α	NO (1π) − NO (1π)	−9.381	9.9	60.4	27.7	2.1
53β	NO (1π) − NO (1π)	−10.189	1.4	28.4	67.2	2.9
52β	linear NO (1π)	−10.244	1.8	1.1	95.6	1.5
51β	bent NO (1π)	−10.383	1.7	95.8	1.1	1.4
50β	NO (1π) − NO (1π)	−10.473	2.5	67.9	29.2	0.5
49α	NO (5σ) − Fe (d_{z^2}, sp) − NO (5σ)	−10.617	20.3	28.2	50.5	1
49β	NO (5σ) − Fe (sp, d_{z^2}) − NO (5σ)	−10.758	10	32.4	56.8	0.8
48α	NO (5σ) − Fe (sp, d_{xz}) − NO (5σ)	−10.885	23.2	47.1	28.1	1.6
48β	NO (5σ) − Fe (sp, d_{xz}) − NO (5σ)	−11.094	13.3	51	27.5	8.2
45α	NO ($4\sigma^*$) − NO ($4\sigma^*$)	−14.782	4	40.8	55	0.2
44α	NO ($4\sigma^*$) − NO ($4\sigma^*$)	−15.167	10.4	47.9	33.8	7.9
44β	NO ($4\sigma^*$) − NO ($4\sigma^*$)	−15.738	3.4	50.2	35.2	11.2
43β	NO ($4\sigma^*$) − NO ($4\sigma^*$)	−16.237	4.8	47.7	36.1	11.3
40α	linear NO (3σ)	−28.675	1.5	0.2	98.2	0
39α	bent NO (3σ)	−28.826	1.2	98.5	0.3	0.1
40β	linear NO (3σ)	−29.283	1.5	0.2	98.2	0
39β	bent NO (3σ)	−29.45	1.1	98.5	0.3	0.1

[a] The orbital configuration of NO is $(3\sigma)^2(4\sigma)^2(5\sigma)^2(1\pi)^4(2\pi^*)^1$. [b] The two NO ligands are distinguished by their bending angles with the iron and are described as bent NO (165.9°) and linear NO (172.4°), respectively.

earlier[6,7] in which L-cysteine mediates the destabilization of dinitrosyl iron complexes in proteins to promote the reassembly of a new iron−sulfur cluster. It is most likely that the initial process is a mechanism of NO donation where the coordinated NO groups in DNIC **1** are transferred to NO-acceptor $[(C_4H_8O)Fe(S,S-C_6H_4)_2]^-$, that is, trans nitrosylation between complex **1** and $[(C_4H_8O)Fe(S,S-C_6H_4)_2]^-$ occurs.

The result obtained from this model study also suggests that L-cysteine may act as an NO acceptor (to form RS−NO) to trigger the repair of nitric oxide-modified [2Fe−2S] ferredoxin in the ferredoxin protein purified from *E. coli* cells treated with nitric oxide[6,7] because DNICs have been reported to react with molecular thiols or protein thiols to yield *S*-nitrosothiols.[27] The liberation of NO from dinitrosyl iron complex **1** in the presence (absence) of the NO-receptor reagent, relevant to biological activities, will be exploited in a continuous study.

Experimental Section

Manipulations, reactions, and transfers of samples were conducted under nitrogen according to standard Schlenk techniques or in a glovebox (argon gas). Solvents were distilled under nitrogen from appropriate drying agents (diethyl ether from CaH_2, acetonitrile from $CaH_2-P_2O_5$, methylene chloride from P_2O_5, and hexane and THF from sodium benzophenone) and stored in dried, N_2-filled flasks over 4-Å molecular sieves. Nitrogen was injected through these solvents before use. The solvent was transferred to a reaction vessel via a stainless steel cannula under positive pressure of N_2. The reagents bis(triphenylphosphoranylidene) ammonium chloride, iron pentacarbonyl, sodium nitrite, and elemental sulfur (Lancaster/Aldrich) were used as received. The compound $[PPN][Fe(CO)_3(NO)]$ was synthesized and characterized by published procedures.[28] NO (SanFu, 10% NO + 90% N_2) was passed through an Ascarite II column to remove higher nitrogen oxides.[29] Photolysis reactions were carried out in a 50-mL, water-cooled, quartz reactor equipped with 16 mercury arc 8-W UV lamps (352 nm) outside the reactor. Infrared spectra of the nitrosyl ν(NO) stretching frequencies were recorded on Bio-Rad model FTS-185 and Perkin-Elmer model Spectrum One B spectrophotometers with sealed solution cells (0.1 mm) and KBr windows. UV−vis spectra were recorded on Hewlett-Packard 71 and GBC Cintra 10e spectrophotometers. Analyses of carbon, hydrogen, and nitrogen were obtained with a CHN analyzer (Heraeus).

Preparation of $[PPN][S_5Fe(NO)_2]$ (1) and $[PPN]_2[S_5Fe(\mu-S)_2FeS_5]$ (2). The compounds $[PPN][Fe(CO)_3(NO)]$ (0.4248 g, 0.6

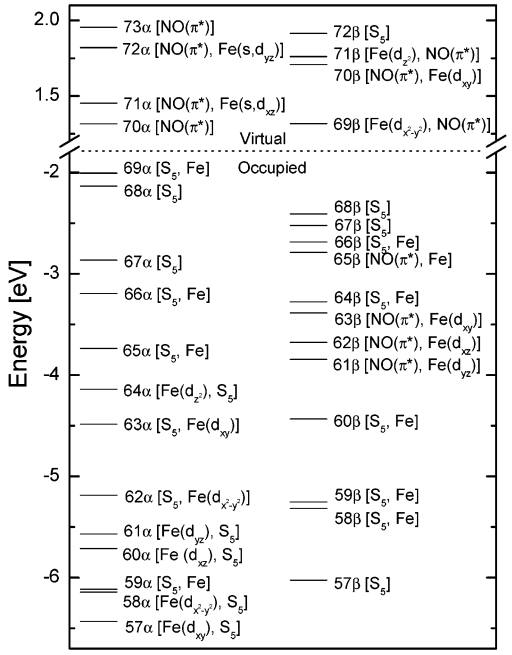

Figure 9. U-B3LYP molecular orbital energy-level diagrams of $[S_5Fe(NO)_2]^-$. The major compositions of MOs are as indicated. The MOs are divided into spin-up (α) levels (left) and spin-down (β) levels (right). The Fermi level is indicated by a dashed line, below which the orbitals are fully occupied and above which lie the unoccupied virtual MOs.

Table 4. Atomic Charge and Spin Together with d-Orbital Occupancies of Fe for Complex **1**

	total charge	total spin	atom	charge	spin	orbital	↑ occ.	↓ occ.	spin
						4s	0.19	0.18	0.01
						d_{xy}	0.93	0.51	0.42
Fe	0.70	2.45				d_{xz}	0.91	0.46	0.45
						d_{yz}	0.93	0.50	0.43
						$d_{x^2-y^2}$	0.96	0.34	0.62
						d_{z^2}	0.93	0.40	0.52
NO (bent)	−0.33	−0.95	N1	−0.03	−0.49				
			O1	−0.30	−0.46				
NO (linear)	−0.29	−0.93	N2	0.00	−0.48				
			O2	−0.29	−0.45				
			S1	−0.44	0.19				
			S2	−0.06	0.02				
sulfur ring	−1.08	0.43	S3	−0.07	0.00				
			S4	−0.06	0.02				
			S5	−0.45	0.20				
total	−1	1		−1	1				

mmol) and S_8 (0.1536 g, 0.6 mmol) were dissolved in 10 mL of THF and stirred overnight under nitrogen at ambient temperature. The reaction was monitored with FTIR. IR spectra (1739 s, 1695 s cm^{-1} (ν_{NO}) (THF)) were assigned to the formation of complex **1**. The resulting mixture was filtered to separate the dark-brown solution (complex **1**) and the reddish-brown solid (complex **2**). The dark-brown THF solution was then concentrated, and diethyl ether was added to precipitate the dark-brown solid $[PPN][(NO)_2FeS_5]$ (**1**) (yield 45% based on total iron). The diffusion of diethyl ether into the THF solution of complex **1** at −15 °C for 4 weeks led to dark-brown crystals suitable for X-ray crystallography. IR (THF): 1739 s, 1695 s (ν_{NO}) cm^{-1}. Absorption spectrum (THF) [λ_{max}, nm (ϵ, M^{-1} cm^{-1})]: 305(10 422), 332(8428), 356(4546), 417(3366), 569(1003). Anal. Calcd for $C_{36}H_{30}N_3O_2P_2S_5Fe$ C, 53.07; H, 3.71; N, 5.16. Found: C, 53.29; H, 3.90; N, 5.58. Acetonitrile was added to extract the reddish-brown solid, and then diethyl ether was slowly added to precipitate the known reddish-brown product $[PPN]_2[S_5Fe(\mu\text{-}S)_2FeS_5]$ (**2**) (yield 40% based on total iron), as identified by X-ray diffraction and UV−vis (absorption spectrum (CH_2Cl_2) [λ_{max}, nm (ϵ, M^{-1} cm^{-1})]: 451(8530), 371(6352)) spectra.[15] Recrystallization by vapor diffusion of diethyl ether into a concentrated CH_3CN solution of complex **2** at −15 °C afforded reddish-brown crystals.

Injection of NO (g) into THF Solution of $[PPN]_2[S_5Fe(\mu\text{-}S)_2FeS_5]$ (2). A heterogeneous THF solution (10 mL) of $[PPN]_2[S_5Fe(\mu\text{-}S)_2FeS_5]$ (**2**) (0.393 g, 0.25 mmol) was injected with NO gas for 20 min at ambient temperature. After the reaction solution was stirred for 3 h, the dark-brown solution was filtered, and the dark-brown product was precipitated by the addition of hexane. The IR (ν_{NO} (THF): 1739 s, 1695 s cm^{-1}) and UV−vis (305-(10 422), 332(8428), 356(4546), 417(3366), 569(1003)) spectra were assigned to the formation of $[PPN][S_5Fe(NO)_2]$ (**1**) (yield 0.250 g, 61%). Recrystallization from saturated THF solution with hexane diffusion gave dark-brown crystals of complex **1**, identified by X-ray diffraction.

Photolysis of THF Solution of Complex 1 and $[PPN][(C_4H_8O)Fe(S,S\text{-}C_6H_4)_2]$. Compounds $[PPN][S_5Fe(NO)_2]$ (**1**) (0.0815 g, 0.1 mmol) and $[PPN][(C_4H_8O)Fe(S,S\text{-}C_6H_4)_2]$ (0.1896 g, 0.2 mmol)[14a] were loaded into a reactor (50 mL), and then 35 mL of THF was added under positive N_2 at ambient temperature. The reaction mixture was then irradiated with a UV lamp (λ = 352 nm) under an N_2 atmosphere at room temperature for 1 h after the reaction solution was stirred in the dark for 30 min. The resulting mixture was filtered to separate the reddish-brown precipitate and the dark reddish-brown upper solution. The reddish-brown precipitate, identified by UV−vis and X-ray diffraction as complex **2**, was isolated in 35% yield (0.028 g) by recrystallization from CH_2Cl_2−diethyl ether−hexane. The filtrate (upper solution) was then monitored with UV−vis. The UV−vis spectra (497, 610, 1190 nm (THF)) indicated the formation of $[PPN][(NO)Fe(S,S\text{-}C_6H_4)_2]$.[14a] The THF solution of complex $[PPN][(NO)Fe(S,S\text{-}C_6H_4)_2]$ was reduced to 5 mL under vacuum, and hexane−diethyl ether was then added to precipitate the dark reddish-brown solid $[PPN][(NO)Fe(S,S\text{-}C_6H_4)_2]$ (0.154 g, 85%) identified by UV−vis (497, 610, 1190 nm (THF)), FTIR (ν(NO): 1789 s cm^{-1} (THF)), and X-ray diffraction.[14a]

X-ray Absorption Measurements. All X-ray absorption experiments were carried out at the National Synchrotron Radiation Research Center (NSRRC), Hsinchu, Taiwan. Both Fe K-edge and O K-edge were recorded at room temperature. For Fe K-edge measurements, the experiment was performed in transmission mode at the BL-17C X-ray Wiggler beamline with a double-crystal Si(111) monochromator. The energy resolution $\Delta E/E$ was estimated to be about 2×10^{-4}. High harmonics were removed by using Rh-coated mirrors. The spectra were scanned from 6.912 to 8.105 keV using a gas ionization detector. A reference Fe foil is always used as an internal standard for the calibration of energy. The ion chambers used to measure the incident (I_0) and transmitted (I) intensities were filled with a mixture of N_2 and He gases and a mixture of N_2 and Ar gases, respectively.

For O K-edge and Fe L-edge absorptions, the data were collected at the 6-m high-energy spherical grating monochromator (HSGM) beamline with 10-μm opening slits, corresponding to ∼0.08- and ∼0.15-eV energy resolution for the O K-edge and Fe L-edge energy ranges, respectively. All samples were ground to powder from single crystals, stuck to a conducting tape, and subjected to an ultrahigh vacuum chamber (10^{-9} Torr). The spectra were recorded in total electron yield mode with a microchannel plate as the detector. Each

spectrum was calibrated by using the known Fe L_{III} edge absorption peak at 708.5 eV of α-Fe_2O_3 and at 531.3 eV by the oxide absorption.

Magnetic Measurements. The magnetization data were recorded on a SQUID magnetometer (MPMS7 Quantum Design company) with an external magnetic field of 1.0 T in the temperature range of 2 to 300 K. The experimental magnetic susceptibility data were corrected for diamagnetism by tabulated Pascal constants.

EPR Measurements. EPR measurements were performed at X band using a Bruker EMX spectrometer equipped with a Bruker TE102 cavity and a Bruker VT2000 temperature control unit (120−300 K). For liquid-helium temperature measurements, an Oxford ESR910 continuous flow cryostat (4−200 K) was used. X-band EPR spectra of complex **1** frozen in THF were obtained with a microwave power of 5 mW, a frequency of 9.4323 GHz (Figure 3A (top)), and a modulation amplitude of 0.05 mT at 100 kHz (temperature = 77 K). X-band EPR spectra (Figure 3B (bottom)) of complex **1** was measured at frequency of 9.78410 GHz at room temperature.

Crystallography. Crystallographic data of complex **1** are summarized in Table 2 and in Supporting Information. The crystal of **1** chosen for the X-ray diffraction study is 0.25 × 0.20 × 0.20 mm^3 in size and was mounted on a glass fiber. Diffraction measurements of complex **1** were carried out at 150(1) K on a Bruker-Nonius Kappa CCD diffractometer with graphite-monochromated Mo K_α radiation (λ = 0.7107 Å). Data were collected with θ in the range of 1.45 to 27.50°. The least-squares refinement on the positional and anisotropic thermal parameters of all nonhydrogen atoms was based on F^2. Absorption correction was made using SORTAV.[30] The program SHELXTL[31] was employed for the structural analyses.

XANES Simulation. The X-ray absorption near-edge spectrum (XANES) of the Fe K-edge was simulated using FEFF82 code[32] on the basis of the full multiple scattering (FMS) applying self-consistent muffin-tin potentials. The energy-dependent exchange-correlation potential of the Hedin−Lungdqvist model was used. The atomic coordinates used in the input file of Atoms-3.0beta9[33] are taken from the crystal structure for the FEFF calculation. A series of computations with increasing the cluster size, from the smallest one with 5 atoms to the largest one with 180 atoms, were performed, and no significant differences were found within the calculated near-edge features. The one reported here includes 47 atoms with a −0.1-eV shift of the Fermi level as well as a reduction of 0.1-eV line broadening.

Computational Details. All calculations were performed at the hybrid HF-DFT functional UB3LYP level with the 6-311++G-(3d, 2p) basis using a tight convergence criterion, as implemented in the Gaussian 98 program package. The geometry of molecule $[S_5Fe(NO)_2]$ is taken from the crystal structure, and no geometric optimization was employed.

Acknowledgment. We thank the National Science Council (Taiwan) for supporting this work. The insight of M. Y. Darensbourg (Texas A&M University) is greatly appreciated.

Supporting Information Available: X-ray crystallographic file in CIF format for the structure determination of $[PPN][S_5Fe(NO)_2]$. This material is available free of charge via the Internet at http://pubs.acs.org.

IC0494915

(33) Ravel, B. *J. Synchrotron Radiat.* **2001**, *8*, 314.